

CFD Analysis on MAV NACA 2412 Wing in High Lift Take-Off Configuration for Enhanced Lift Generation

Arvind Prabhakar* and Ayush Ohri

Department of Mechanical and Manufacturing Engineering, Manipal Institute of Technology, Karnataka, India

Abstract

In a high lift take off configuration an MAV wing utilizes partially extended flaps and slats. Slats and Flaps are high lift devices installed on a wing for the purpose of augmenting Coefficient of Lift (C_L). While Slats are installed on the leading edge of a wing the Flaps may be installed on the trailing edge or the leading edge of a wing. In this paper the effect of Slot size created by the Slats in percentage of wing chord 'c' and Double Slotted Flaps on C_L for a MAV NACA 2412 has been studied using CFD analysis at 2×10^5 Reynolds Number. It is found that the maximum value of C_L achieved is 67.134% higher than the plain NACA 2412 wing at 4 degrees angle of attack when slats are extended at 1.7 percent of wing chord 'c'. The Stall angle of the MAV NACA 2412 wing in high lift take-off configuration was found to be 54 degrees whereas the plain NACA 2412 wing stalled at 20 degrees angle of attack.

Keywords: Angle of attack; Augmentation; Computational fluid dynamics

Abbreviations: NACA: National Advisory Committee on Aeronautics; MAV: Micro Air Vehicle; CFD: Computational Fluid Dynamics; C_L : Coefficient of Lift; (c): Wing Chord Slats; DSP: Double Slotted Flaps; Slot; Stall Angle

Nomenclature

C_L -Coefficient of Lift

'c'-wing chord

d-Perpendicular slat distance from a point on the airfoil nose

L/D-Lift to drag ratio

Introduction

Flaps are high lift devices attached to the leading or trailing edge of a wing. They help to increase the value of C_L and the Stall Angle during the take-off phase of an aircraft. Stall Angle is the angle between the chord line of an airfoil and the undisturbed relative airflow at which stalling occurs where stalling refers to the condition when there is a sudden reduction in the lift generated by the wing [1,2]. If the stalling angle is higher compared to plain airfoils it allows the aircraft to take off at lower speeds and hence it can even take off from shorter runways [3].

Flaps when fully extended during the landing phase of an aircraft tend to increase the drag so that the aircraft can land on the runway with a safe speed depending upon the shape, size and weight of the aircraft [4]. In this paper application of flaps during take-off phase has been highlighted.

Slats are referred to as high lift devices which are attached to the leading edge of a wing. Their function is similar to that of the flaps. They help in increasing the coefficient of lift and stalling angle by re-energizing the airflow over the wings surface so that the airflow remains streamline upto high angles of attack. However, it may start becoming turbulent at much higher angles. Once the aircraft takes-off and begins to cruise at a particular altitude the slats and flaps are made to retract back into the leading and trailing edges of the wing. If the slats and flaps remain extended from the wing during the cruise period of the aircraft they tend to increase the drag produced and thereby increase the fuel consumption of the aircraft [5].

Flaps are of various types such as plain flaps, split flaps, fowler flaps, slotted flaps, double slotted flaps, zap flaps, Krueger flaps etc. The type of flap that needs to be used for a particular aircraft depends upon size, speed and shape of the aircraft. Generally in modern day jetliners Krueger flaps are used which are attached to the leading edge of the wing.

It has been investigated that the lift of a MAV can be enhanced by using moveable passive flaps at the extrado of the airfoil at low Reynolds number of about 3×10^4 and it was found that the lift of an SD8020 airfoil wing increased by 50% [6]. In this paper double slotted flaps and slats were attached to the wing of a micro air vehicle and their effect was studied. The plain NACA 2412 wing was 6 inches in chord and it had a span of 12 inches which is ideally suitable for a MAV. The chord of flap was 25 percent of the plain NACA 2412 wing. The analysis was carried out at 2×10^5 Reynolds Number. Standard K-epsilon turbulence model was used to carry out CFD simulation. The results obtained were compared with the results of plain wing at different angles of attack. In armin ghoddoussi's, conceptual study of airfoil performance enhancements it has been proved that at slot size equal to 1.7% of wing chord 'c' maximum amount of lift is generated [7]. In this paper the comparison of results in terms of CL and stall angle proved that the wing which had slat extended by distance 'd' equal to 1.7 percent of plain NACA 2412 wing chord and double slotted flap extended at an angle of 40 degrees generated maximum value of CL. hence, this configuration was assumed as the MAV NACA 2412 high lift take off configuration (Figure 1).

*Corresponding author: Arvind Prabhakar, Department of Mechanical and Manufacturing Engineering, Manipal Institute of Technology, Karnataka, India, Tel: 08202571060; E-mail: arvind.prabhakar1988@gmail.com

Received September 16, 2013; Accepted November 27, 2013; Published December 04, 2013

Citation: Prabhakar A, Ohri A (2013) CFD Analysis on MAV NACA 2412 Wing in High Lift Take-Off Configuration for Enhanced Lift Generation. J Aeronaut Aerospace Eng 2: 125. doi:10.4172/2168-9792.1000125

Copyright: © 2013 Prabhakar A, et al. This is an open-access article distributed under the terms of the Creative Commons Attribution License, which permits unrestricted use, distribution, and reproduction in any medium, provided the original author and source are credited.

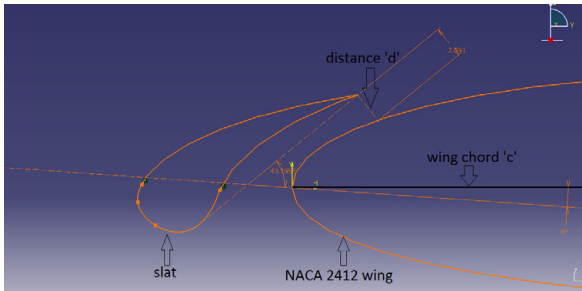


Figure 1: MAV NACA 2412 slot nomenclature.

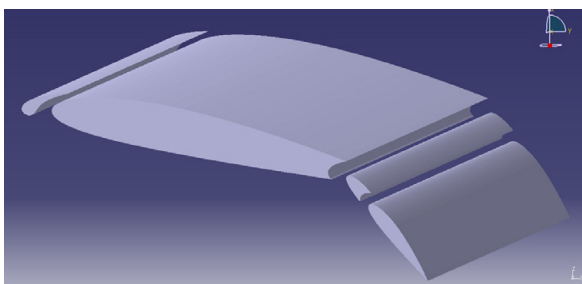


Figure 2: 3d modeling of the MAV NACA 2412 wing on CATIA v5.

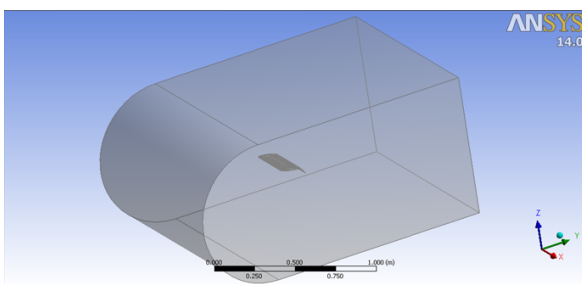


Figure 3: Design of fluid domain and Boolean subtraction on ANSYS workbench.

Theoretical Formulation and Method of Solution

The objective of the analysis is to study the effect of Slot size in percentage of wing chord 'c' as a measure of high lift take-off configuration. The following assumptions are made during the analysis.

- The computational domain is assumed to be made of solid-air interface.
- Turbulent flow is assumed under fully developed conditions.
- Solution is reached at steady state which is assumed to be obtained after all the residuals are brought to prescribed constant values.

Methodology

The methodology for computation involved the designing of plain NACA2412 airfoils, slats, double slotted flaps and a bullet shaped fluid domain on commercial cad software CATIA V5. The meshing of the designs for grid generation was done on ICEM CFD ANSYS 14.0 workbench. The CFD analysis was carried out using commercial code ANSYS FLUENT 14.0. The post processing of the results was done using ANSYS CFD POST.

Design of MAV NACA 2412 airfoil

The 2D airfoil co-ordinates were exported to part module of CATIA V5 which is a commercial bench marked software for modeling. The 2d airfoil coordinates sketch was extruded using the pad command. The slat is of NACA 2415 profile and the airfoil and flaps are of NACA 2412 profile (Figure 2).

Design of fluid domain

A bullet shaped fluid domain was created in part design module of CATIA V5 to replicate the experimental wind tunnel whose results have been used to validate the CFD analysis (Figure 3).

Grid generation

Tetrahedral meshing was done for generating the grid. Refinements were done on the leading and trailing edges of the airfoil, slats and double slotted flaps. Coarse type sizing was used to generate the mesh. Since tetrahedral meshing takes lesser computational time and keeps the accuracy of the results obtained after analysis within acceptable limits, it was used for generating the grid. The Minimum Size was set to 0.0018 whereas the Maximum Size, Maximum Face size and Growth Rate were set to 3 meters, 3 meters, 1.072 respectively. The Minimum Edge Length was set to 7.8474×10^{-5} .

The mesh quality depends upon the value of smoothness which defines the rate of change of cell size. For a good quality mesh the rate of change of cell size should be smooth. The value of smoothness has been set to medium to ensure a good quality mesh (Figure 4).

Grid Generation Outline

After the wing had been accurately modeled in CATIA V5 as per the dimensions, a 3D grid was generated on the modeled wing which divides the volume surrounding the wing into several smaller volumes. The type of grid layout that was generated on different areas of the wing depended upon the type of test the grid was required to solve. Since the air flow whose behavior had to be studied in order to study the phenomenon of turbulence was majorly stuck to the upper portion of the wing, grid with high cell density was generated on the upper surface of the wing. Since substantial amount of air causing re-energization of turbulent flow over the upper surface of the wing passes through slot and the gap between the main wing and the double slotted flaps, the leading and trailing edges of the slats, flaps and wing were refined with a Minimum size of 0.0018 m to generate a grid of very high cell density so that the phenomenon of re-energisation could be studied (Figure 5). Shows grid generation outline.

The Standard K-epsilon model is one of the most common Turbulence model used in CFD analysis. This is a 2 equation model

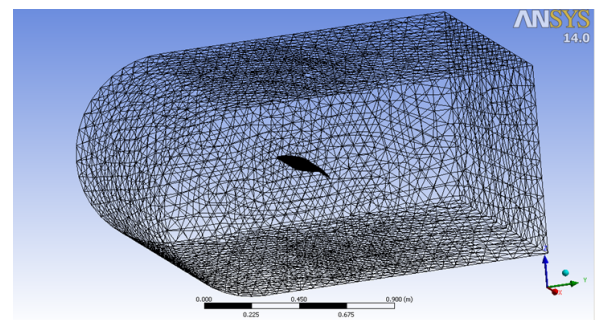


Figure 4: Generation of grid on ICEM CFD.

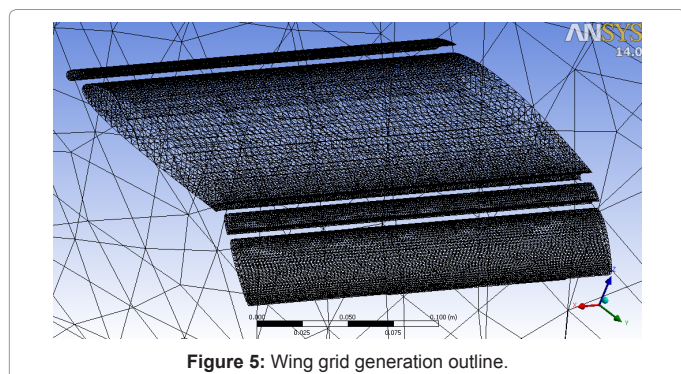


Figure 5: Wing grid generation outline.

which represents the turbulent properties of flow. This model takes into account the effect of convection and diffusion of turbulent flow. The first equation gives the turbulent kinetic energy of the flow which is represented by symbol K whereas the second equation gives the turbulent dissipation in the flow which is represented by symbol ϵ . This model does not give accurate results in case the pressure gradients are large and is mainly used in case of free-shear layer flows with relatively small pressure gradients.

First order upwind scheme is selected for spatial discretization of the Reynolds Average Navier Stoke (RANS) equations as well as energy and turbulence equations [8,9]. Converged results are obtained after the residuals were found to be less than the specified values. A converged result renders an energy residual of 10^{-6} and momentum and turbulence kinetic energy residuals being 10^{-5} [9].

Turbulent Kinetic Energy Equation

Turbulence dissipation equation

$$\frac{\delta(\rho \epsilon)}{\delta t} + \frac{\delta(\rho \epsilon u_i)}{\delta x_i} = \frac{\delta}{\delta x_j} \left[\frac{\mu_t}{\sigma_k} \frac{\delta k}{\delta x_j} \right] + C_{1\epsilon} \frac{\epsilon}{k} 2\mu_t E_{ij} - C_{2\epsilon} \rho \frac{\epsilon^2}{k}$$

u_i represents velocity component in corresponding direction

E_{ij} component of rate of deformation

μ_t represents eddy viscosity

$$\mu_t = \rho C_\mu \frac{k^2}{\epsilon}$$

Grid independence test

A grid independence test was carried out to ensure that there is no effect on the solution due to the size of the grid and to study the effect of quality of mesh on accuracy of solution. This was achieved by considering three different grid configurations and studying their convergence behavior for the values of coefficient of lift at Reynolds Number 2×10^5 .

Grid configuration 1 was a coarse grid that had 513211 numbers of cells and a Minimum Orthogonal Quality=0.0485750 it showed inaccurate results due to a deviation of about 15.36% from the experimental value.

Grid configuration 2 was finer grid that had 2853877 number of cells with Minimum Orthogonal Quality=0.18607 it consisted of refinement at the leading and trailing edges of the wing, this showed realistic behavior and solution obtained was closer to the experimental data. A deviation of about 4.41% was observed.

Grid configuration 3 was the finest mesh and had 4217840 number of cells with a Minimum Orthogonal Quality=0.188692 and showed a behavior not much different than configuration 2 and also, produced a solution similar to configuration 2 hence, grid configuration 2 was selected for all further analysis, considering computation time and size constraints in mind. The plot of solutions obtained with these three different grid configurations and experimental results has been shown in Figure 6.

Validation of the predicted values from CFD Analysis

for the purpose of CFD validation The values obtained from the CFD Analysis of the plain NACA 2412 wing at Reynolds Number 2×10^5 for angles of attack 0, 4, 8, 12, 16, and 18 degrees were compared with the experimental results from the wind tunnel data on the airfoil of similar dimensions and profile at the same Reynolds Number [9].

It can be observed from figure 4 that the values of C_L obtained are in good agreement with the experimental values [9] hence, this has enabled the analysis to be extended for the analysis on MAV NACA 2412 wing in high take off configuration for predicting the values of C_L (Figure 7).

Once the CFD analysis results were obtained for the 3D wing with flaps and slats attached to it, a comparison on the basis of the values of C_L and Lift to Drag ratio (L/D) obtained for various angles of attack was made. Moreover the value of Stall Angle obtained in case of plain MAV NACA2412 wing was lesser compared to that of MAV NACA2412 wing having slats and flaps attached to it. The simulation was carried out at a Reynolds Number of 2×10^5 which corresponded to a velocity of 20.5826 m/s. The values of C_L and L/D ratio were calculated at 4, 8, 12,

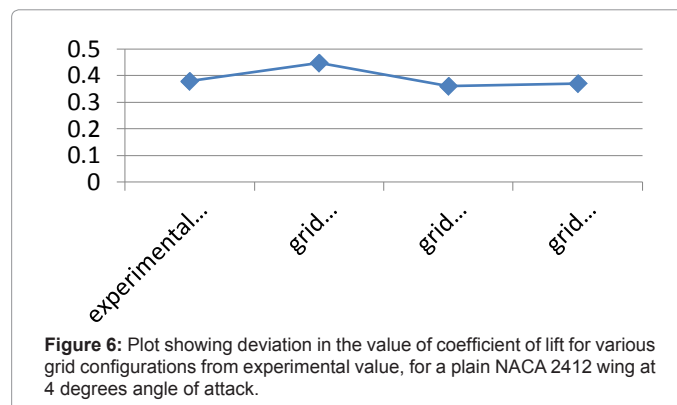


Figure 6: Plot showing deviation in the value of coefficient of lift for various grid configurations from experimental value, for a plain NACA 2412 wing at 4 degrees angle of attack.

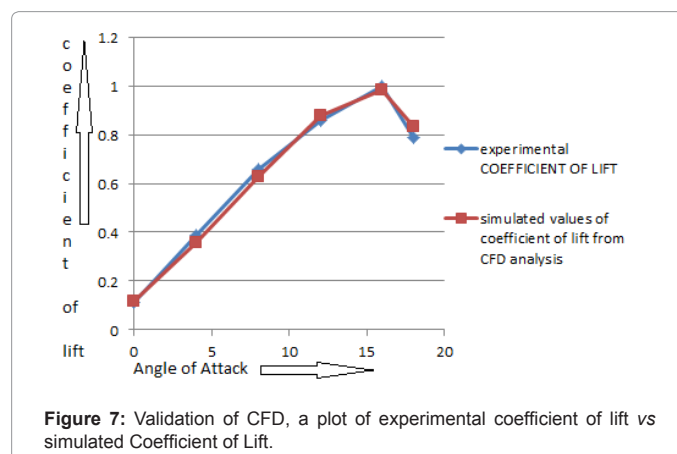


Figure 7: Validation of CFD, a plot of experimental coefficient of lift vs simulated Coefficient of Lift.

18 and 20 degrees angle of attack for the plain MAV wing. Whereas the C_L and L/D ratio values for the MAV wing with flaps and slats attached to it was calculated at 4, 8, 12, 16, 18, 20, 22, 24, 26, 30, 34, 38, 42, 46, 50 and 54 degrees angle of attack. It was observed from the values of C_L obtained after CFD simulation that the plain NACA 2412 wing began to stall at 20 degrees whereas the MAV wing having flaps and slats attached to it began to stall at 54 degrees angle of attack. All the analysis were carried out with double slotted flaps extended at 40 degrees since it corresponded to high take off configuration. Armin ghoddoussi in his conceptual study of airfoil performance enhancements studied and proved that at slot size equal to 1.7% of wing chord 'c' maximum amount of lift is generated [8]. In consideration of this aspect the present paper extends the work to study the additional effect of double slotted flaps at 40 degrees attached to the MAV NACA 2412 wing. A study on the slat gap size when extended at 0.5%, 1.2%, 1.7%, 3.2%, 3.7%, 4.2% and 4.7% of plain MAV NACA 2412 wing chord was done to obtain maximum value of C_L . It was observed that when slats were extended at 1.7% of plain MAV NACA 2412 wing chord with double slotted flaps attached to the wing extended at 40 degrees, maximum value of C_L was obtained.

Lift-coefficient analysis

Angle of attack 4°: At 2×10^5 Reynolds Number the value of C_L for MAV NACA 2412 wing with a configuration of slot size equal to 1.7% wing chord 'c' and double slotted flaps extended at 40 degrees was found to be 0.600765 which was the maximum value of C_L obtained in comparison to the C_L values obtained with 0.5%, 1.2%, 3.2%, 3.7%, 4.2%, 4.7% slot size configuration, this value of C_L obtained was found to be higher by 67.134% compared to plain NACA 2412.

Angle of attack 8°: At 2×10^5 Reynolds Number the value of C_L for MAV NACA 2412 wing with a configuration of slot size equal to 1.7% wing chord 'c' and double slotted flaps extended at 40 degrees was found to be 0.80005 which was the maximum value of C_L obtained in comparison to the C_L values obtained with 0.5%, 1.2%, 3.2%, 3.7%, 4.2%, 4.7% slot size configuration, this maximum value of C_L was found to be higher by 27.349% compared to plain NACA 2412.

Angle of attack 12°: At 2×10^5 Reynolds Number the value of C_L for MAV NACA 2412 wing with a configuration of slot size equal to 1.7% of wing chord 'c' and double slotted flaps extended at 40 degrees was found to be 1.052494 which was the maximum value of C_L obtained in comparison to the C_L values obtained with 0.5%, 1.2%, 3.2%, 3.7%, 4.2%, 4.7% slot size configuration, this maximum value of C_L obtained was found to be higher by 19.889% compared to plain NACA 2412.

Angle of attack 16°: At 2×10^5 Reynolds Number the value of C_L for MAV NACA 2412 wing with a configuration of slot size equal to 1.7% of wing chord 'c' and double slotted flaps extended at 40 degrees was found to be 1.254877 which was the maximum value of C_L obtained in comparison to the C_L values obtained with 0.5%, 1.2%, 3.2%, 3.7%, 4.2%, 4.7% slot size configuration.

Angle of attack 18°: At 2×10^5 Reynolds Number the value of C_L for MAV NACA 2412 wing with a configuration of slot size equal to 1.7% of wing chord 'c' and double slotted flaps extended at 40 degrees was found to be 1.355955 which was the maximum value of C_L obtained in comparison to the C_L values obtained with 0.5%, 1.2%, 3.2%, 3.7%, 4.2%, 4.7% slot size configuration (Figures 8-13) (Table 1).

Effect of MAV NACA 2412 wing on stall angle

At 2×10^5 Reynolds Number it was found that the MAV NACA

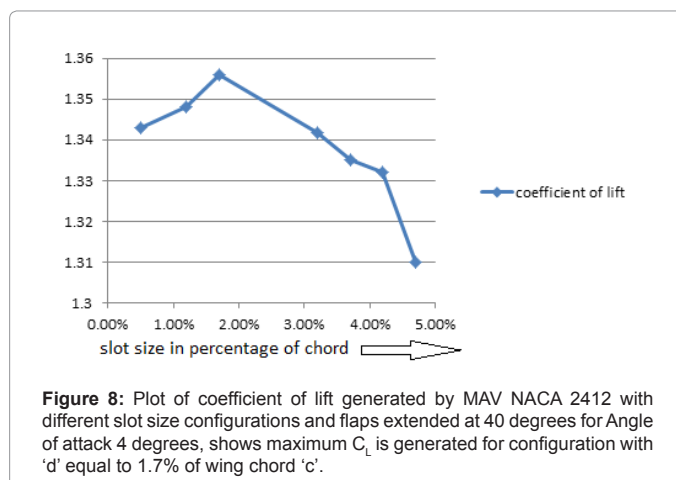


Figure 8: Plot of coefficient of lift generated by MAV NACA 2412 with different slot size configurations and flaps extended at 40 degrees for Angle of attack 4 degrees, shows maximum C_L is generated for configuration with 'd' equal to 1.7% of wing chord 'c'.

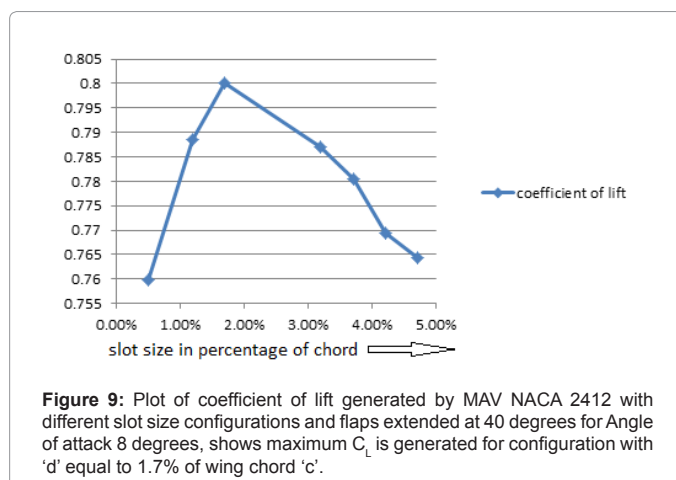


Figure 9: Plot of coefficient of lift generated by MAV NACA 2412 with different slot size configurations and flaps extended at 40 degrees for Angle of attack 8 degrees, shows maximum C_L is generated for configuration with 'd' equal to 1.7% of wing chord 'c'.

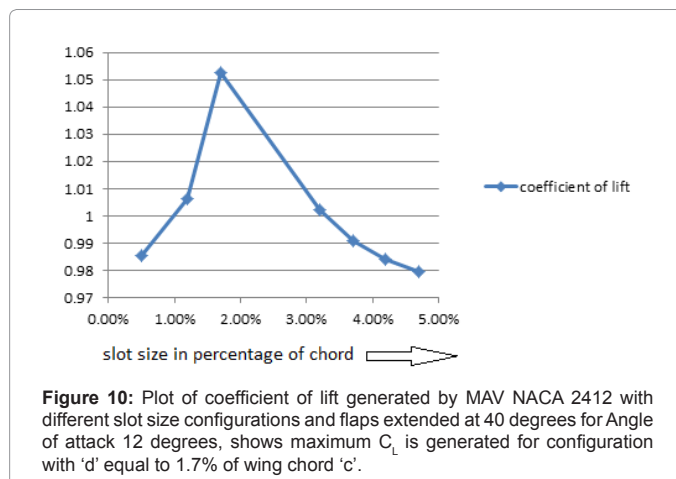


Figure 10: Plot of coefficient of lift generated by MAV NACA 2412 with different slot size configurations and flaps extended at 40 degrees for Angle of attack 12 degrees, shows maximum C_L is generated for configuration with 'd' equal to 1.7% of wing chord 'c'.

2412 wing with 'd' equal to 1.7% of wing chord 'c' and double slotted flaps extended at an angle of 40 degrees increased stalling angle upto 54 degrees compared to a stalling angle of 18 degrees achieved by plain NACA 2412 airfoil of same aspect ratio (Table 2).

Lift to Drag (L/D) ratio analysis

Angle of attack 4°: at 2×10^5 Reynolds Number the value of L/D ratio for high lift configuration with 'd' equal to 1.7% of wing chord 'c'

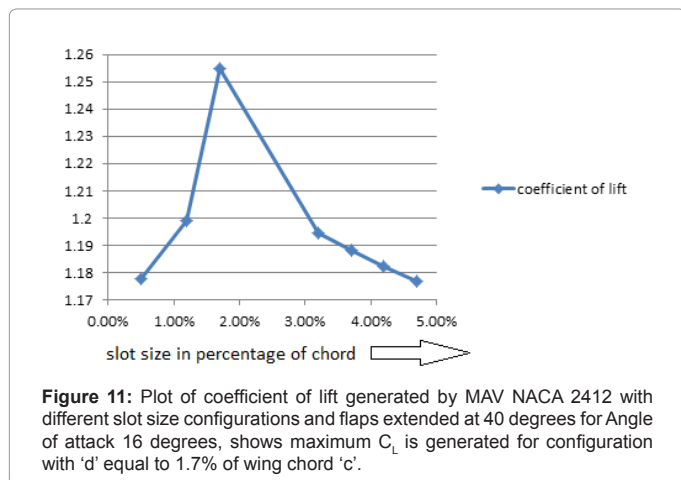


Figure 11: Plot of coefficient of lift generated by MAV NACA 2412 with different slot size configurations and flaps extended at 40 degrees for Angle of attack 16 degrees, shows maximum C_L is generated for configuration with 'd' equal to 1.7% of wing chord 'c'.

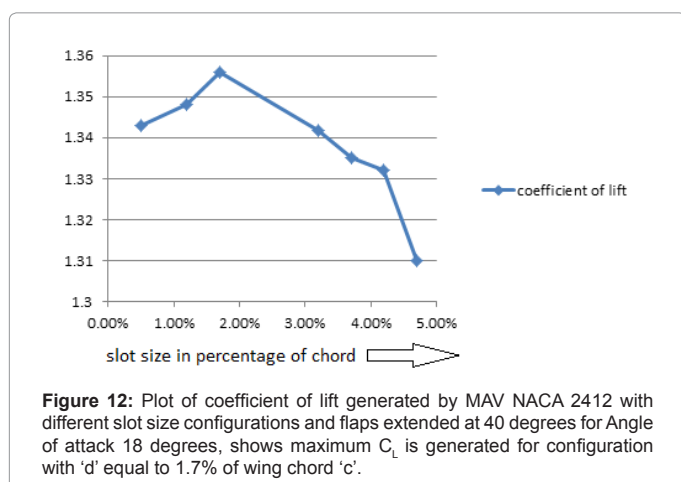


Figure 12: Plot of coefficient of lift generated by MAV NACA 2412 with different slot size configurations and flaps extended at 40 degrees for Angle of attack 18 degrees, shows maximum C_L is generated for configuration with 'd' equal to 1.7% of wing chord 'c'.

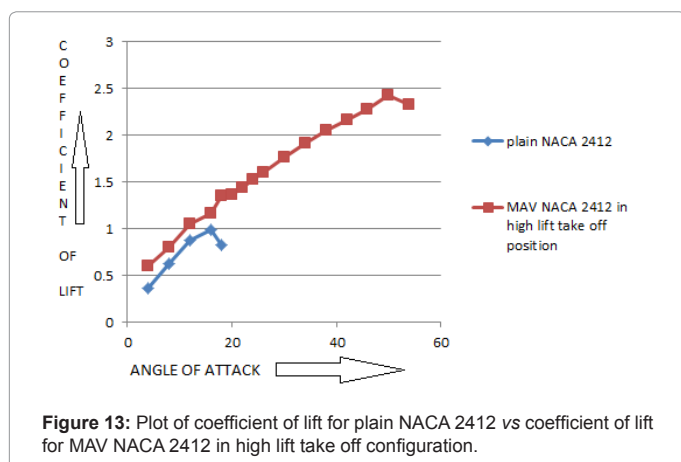


Figure 13: Plot of coefficient of lift for plain NACA 2412 vs coefficient of lift for MAV NACA 2412 in high lift take off configuration.

and double slotted flaps extended at 40 degrees obtained was 2.2981 which is 77.3429% lower than the plain NACA 2412 wing (Table 3).

Angle of attack 8°: at 2×10^5 Reynolds Number the value of L/D ratio for high lift configuration with 'd' equal to 1.7% of wing chord 'c' and double slotted flaps extended at 40 degrees obtained was 2.3686 which is 77.1193% lower than the plain NACA 2412 wing.

Angle of attack 120°: at 2×10^5 Reynolds Number the value of L/D ratio for high lift configuration with 'd' equal to 1.7% of wing chord 'c'

Angle of Attack (In Degrees)	Coefficient of Lift (C_L)						
	MAV NACA 2412 With d=5% of CHORD 'C'	MAV NACA 2412 With d=2% of CHORD 'C'	MAV NACA 2412 With d=1.7% of CHORD 'C'	MAV NACA 2412 With d=3.2% of CHORD 'C'	MAV NACA 2412 With d=3.7% of CHORD 'C'	MAV NACA 2412 d=4.2% of CHORD 'C'	MAV NACA 2412 With d=4.7% of CHORD 'C'
4	0.525731	0.578133	0.600765	0.576324	0.58268	0.566233	0.564747
8	0.759913	0.788417	0.80005	0.78697	0.780398	0.769281	0.764446
12	0.985432	1.006522	1.052494	1.002013	0.990952	0.984119	0.979466
16	1.177815	1.198905	1.254877	1.194396	1.188335	1.182502	1.176849
18	1.343061	1.348144	1.355955	1.341745	1.335	1.332122	1.310071

Table 1: Lift Coefficient comparison for various wing configurations, Reynolds Number= 2×10^5 .

Wing Configuration	Coefficient of Lift				
	4°	8°	12°	16°	18°
Plain NACA 2412	0.35945018	0.62823054	0.87788515	0.983365	0.83125631
MAV NACA 2412 In High Lift Take Off Configuration	0.600765	0.80005	1.052494	1.194396	1.341745

Table 2: Lift Coefficient comparison between plain NACA 2412 and MAV NACA 2412 with 'd' equal to 1.7% of chord 'c' and flaps extended at 40 degrees (i.e. MAV NACA 2412 in high lift take off configuration) at Reynolds Number= 2×10^5 .

Angle of Attack (In Degrees)	Plain NACA 2412	MAV NACA 2412 In High Lift Take Off Configuration
4	0.35945018	0.60076541
8	0.62823054	0.800504
12	0.87788515	1.0524937
16	0.983365	1.1648765
18	0.83125631	1.3559547
20	STALL.	1.3644363
22		1.4416201
24		1.5277626
26		1.599189
30		1.7714788
34		1.9146608
38		2.0519581
42		2.1697813
46		2.276407
50		2.4338166
54		2.329211
55		STALL.

Table 3: Stall angle determination by Lift Coefficient comparison between plain NACA 2412 and MAV NACA 2412 with 'd' equal to 1.7% of wing chord 'c' and flaps extended at 40 degrees (i.e. MAV NACA 2412 in high lift take off configuration) at Reynolds Number= 2×10^5 .

and double slotted flaps extended at 40 degrees obtained was 2.0998 which is 76.109% lower than the plain NACA 2412 wing.

Angle of attack 16°: at 2×10^5 Reynolds Number the value of L/D ratio for high lift configuration with 'd' equal to 1.7% of wing chord 'c' and double slotted flaps extended at 40 degrees obtained was 2.1083 which is 78.1281% lower than the plain NACA 2412 wing.

Angle of attack 18°: at 2×10^5 Reynolds Number the value of L/D ratio for high lift configuration with 'd' equal to 1.7% of wing chord 'c' and double slotted flaps extended at 40 degrees obtained was 2.12810 which is 79.3441% lower than the plain NACA 2412 wing (Table 4).

Contours of coefficient of pressure

The plot of Coefficient of Pressure for a MAV NACA 2412 wing

Wing Configuration	LIFT/DRAG RATIO				
	4°	8°	12°	16°	18°
Plain Rectangular NACA 2412	10.143	10.352	8.864	9.639	10.30
MAV NACA 2412 In High Lift Take Off Position	2.2981	2.3686	2.099	2.1083	2.128

Table 4: LIFT TO DRAG ratio comparison between plain NACA 2412 and MAV NACA 2412 in high lift take off configuration.

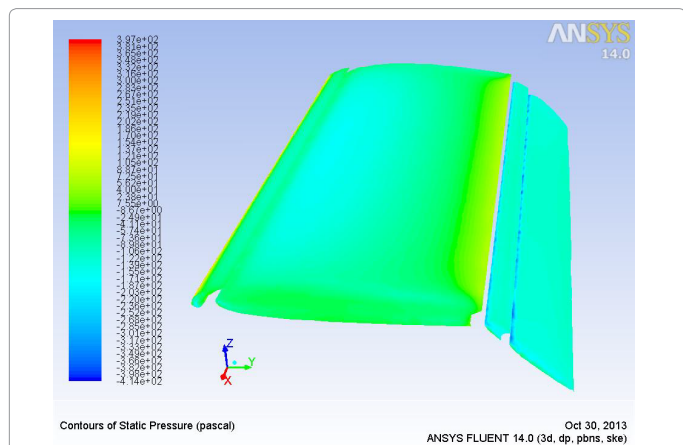


Figure 14: Top surface Coefficient of Pressure contours on MAV NACA 2412 wing at Angle of Attack 4 degrees with 'd' equal to 1.7% of wing chord (c) and double slotted flaps extended at 40 degrees at Reynolds Number= 2×10^5 .

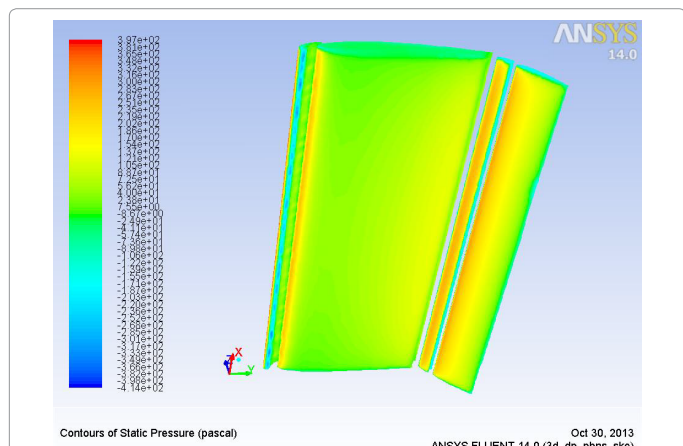


Figure 15: Bottom surface Coefficient of Pressure contours on MAV NACA 2412 wing at Angle of Attack 4 degrees with 'd' equal to 1.7% of wing chord (c) and double slotted flaps extended at 40 degrees at Reynolds Number= 2×10^5 .

with double slotted flaps and slats attached to it is shown from figures 14 to 21. The slats are extended to maximum lift generation position that is 'd' is equal to 1.7% of wing chord (c). The figures suggest that with increasing angle of attack from 4 to 18 degrees the low pressure coefficient area tends to shift towards the leading edge on the upper surface. The magnitude of this Pressure Coefficient is lesser than the Pressure Coefficient on the plain NACA 2412 wing thus, causing higher lift generation. The intensity of this Pressure Coefficient decreases with increasing angle of attack suggesting lower values of Pressure Coefficient and indicating a high lift generation at such positions. The bottom surface contours for coefficient of pressure suggest increasing pressure coefficient at the

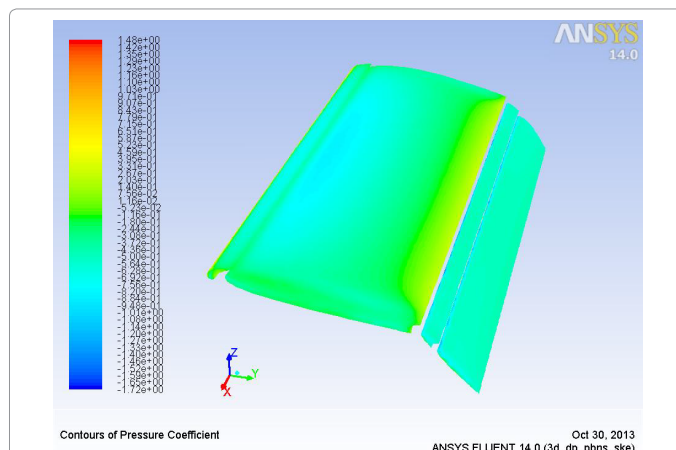


Figure 16: Top surface Coefficient of Pressure contours on MAV NACA 2412 wing at Angle of Attack 8 degrees with 'd' equal to 1.7% of wing chord (c) and double slotted flaps extended at 40 degrees at Reynolds Number= 2×10^5 .

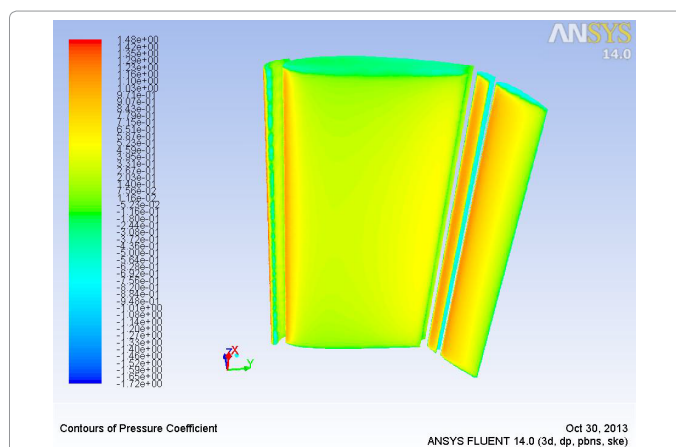


Figure 17: Bottom surface Coefficient of Pressure contours on MAV NACA 2412 wing at Angle of Attack 8 degrees with 'd' equal to 1.7% of wing chord (c) and double slotted flaps extended at 40 degrees at Reynolds Number= 2×10^5 .

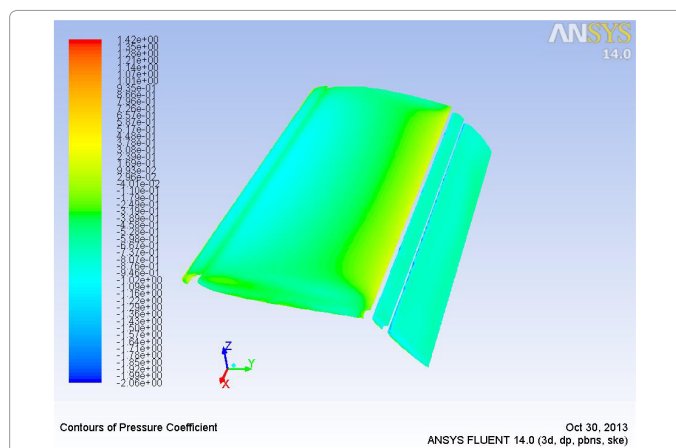


Figure 18: Top surface Coefficient of Pressure contours on MAV NACA 2412 wing at Angle of Attack 12 degrees with 'd' equal to 1.7% of wing chord (c) and double slotted flaps extended at 40 degrees at Reynolds Number= 2×10^5 .

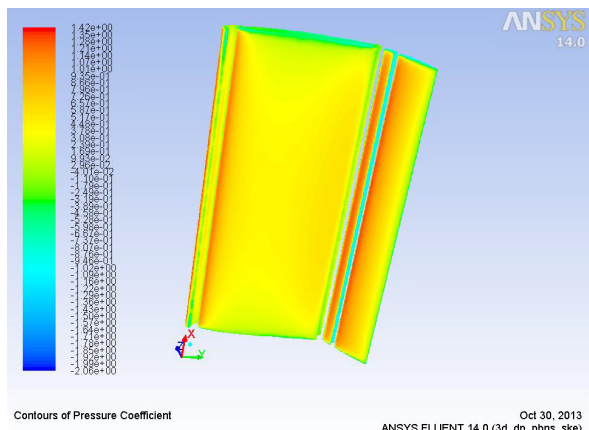


Figure 19: Bottom surface Coefficient of Pressure contours on MAV NACA 2412 wing at Angle of Attack 12 degrees with 'd' equal to 1.7% of wing chord (c) and double slotted flaps extended at 40 degrees at Reynolds Number= 2×10^5 .

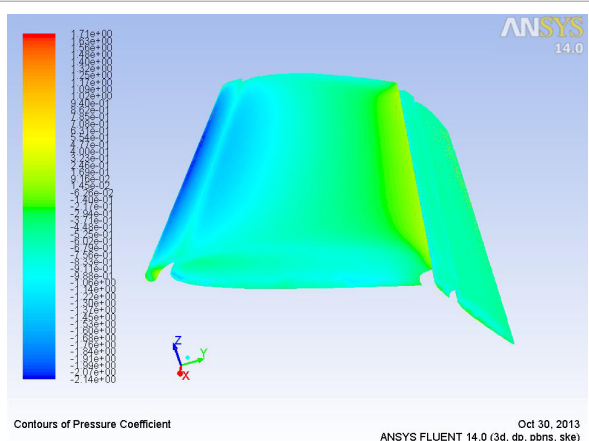


Figure 20: Top surface Coefficient of Pressure contours on MAV NACA 2412 wing at Angle of Attack 18 degrees with 'd' equal to 1.7% of wing chord (c) and double slotted flaps extended at 40 degrees at Reynolds Number= 2×10^5 .

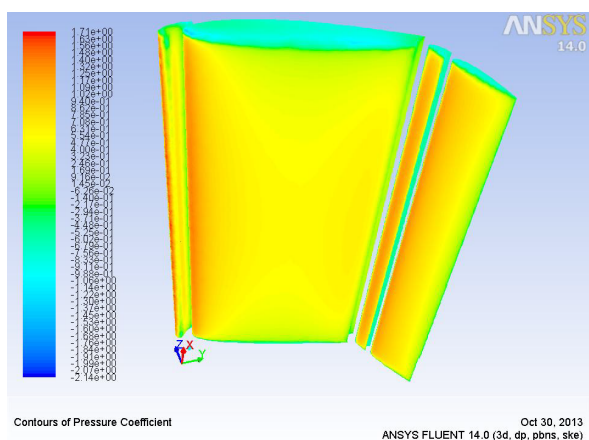


Figure 21: Bottom surface Coefficient of Pressure contours on MAV NACA 2412 wing at Angle of Attack 18 degrees with 'd' equal to 1.7% of wing chord (c) and double slotted flaps extended at 40 degrees at Reynolds Number= 2×10^5 .

Pathlines

Pathlines are used to study the path of a fluid as it moves over a structure or interacts with it. Lines generated during post processing of CFD results individually define the flow path of a fluid on the design. These lines are graphically represented by various colour. Each colour represents a particular magnitude of velocity, pressure, energy etc. The figures below show Pathlines of velocity magnitude. It is observed from the figures 19 to 23 that the turbulent flow in case of plain NACA 2412 wing as shown in figure 19 gets shifted towards the trailing edge of the airfoil and on the top surface of double slotted flaps of MAV NACA 2412 wing in high lift configuration as shown in figure 20. Therefore the flow over the wing portion of the MAV NACA 2412 wing becomes laminar and gives a higher value of CL and increases Stall angle in comparison to the plain NACA 2412 wing. The shift of turbulent flow takes place in case of MAV wing due to re-energization phenomenon which occurs through gap size created by the slats and double slotted flaps shown in Figure 21 to Figure 25 respectively [8]. Generally in this phenomenon bleed air from engine exhaust is made to pass over the rear upper surface of the wing and flaps through the gaps created by the flaps and slats. This air allows the air flow to remain attached to the wings surface at even higher angles of attack causing the Stall angle to rise considerably [8].

Conclusion

The results obtained from the CFD analysis of various wing

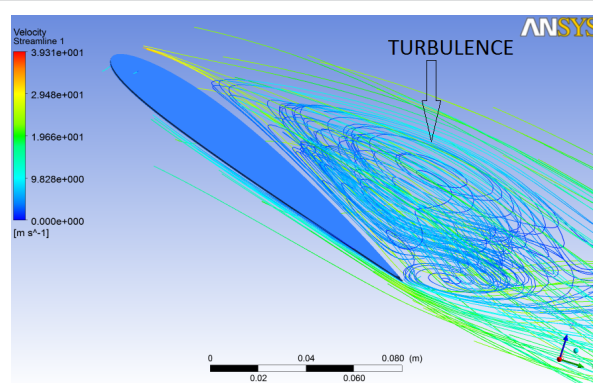


Figure 22: Pathlines of velocity magnitude on plain NACA 2412 airfoil at Angle of Attack 18 degrees at Reynolds number= 2×10^5 showing high turbulence.

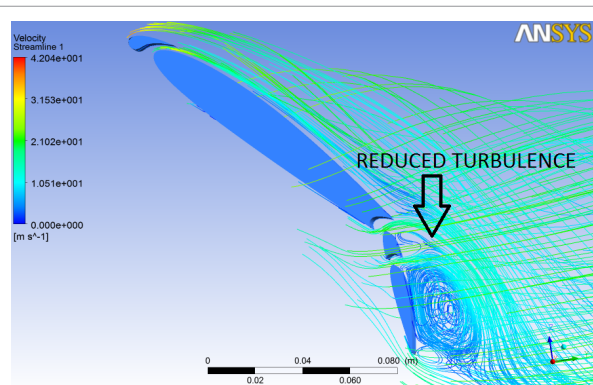


Figure 23: Pathlines of velocity magnitude on MAV NACA 2412 airfoil at Angle of Attack 50 degrees with 'd' equal to 1.7% of wing chord and flaps extended at 40 degrees at Reynolds number= 2×10^5 .

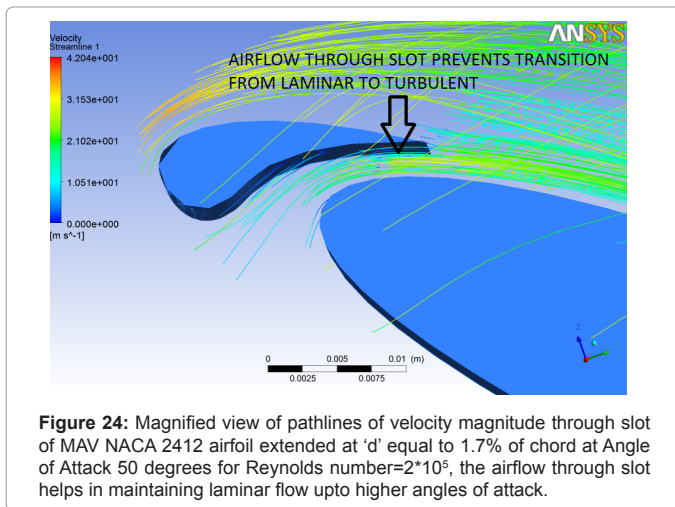


Figure 24: Magnified view of pathlines of velocity magnitude through slot of MAV NACA 2412 airfoil extended at 'd' equal to 1.7% of chord at Angle of Attack 50 degrees for Reynolds number= 2×10^5 , the airflow through slot helps in maintaining laminar flow upto higher angles of attack.

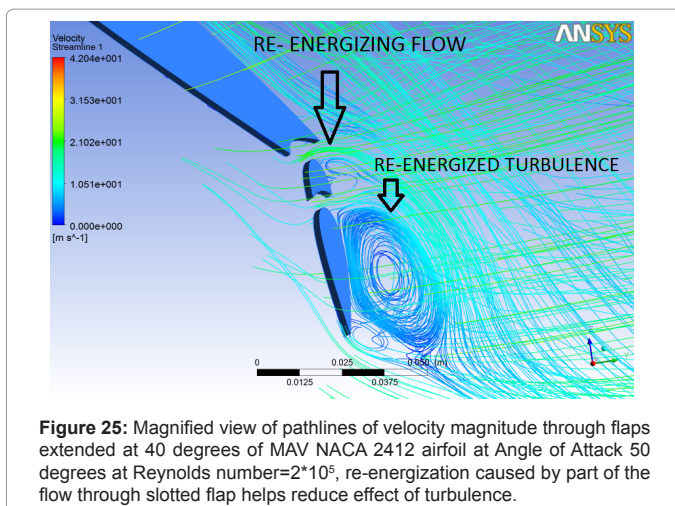


Figure 25: Magnified view of pathlines of velocity magnitude through flaps extended at 40 degrees of MAV NACA 2412 airfoil at Angle of Attack 50 degrees at Reynolds number= 2×10^5 , re-energization caused by part of the flow through slotted flap helps reduce effect of turbulence.

configurations proved that the wing configuration having 'd' equal to 1.7% of wing chord and double slotted flaps extended to 40 degrees was the ideal MAV high lift take-off configuration. The Stalling Angle that was obtained from this MAV high lift take-off wing configuration was 54 degrees while that of plain NACA 2412 wing was 20 degrees this proved that the MAV could sustain lift at much higher angles of attack in comparison to the plain NACA 2412 wing.

References

1. Burke R (2005) Principles of Flight.
2. http://en.wikipedia.org/wiki/Stall_%28flight%29
3. http://www.faa.gov/regulations_policies/handbooks_manuals/aviation/pilot_handbook/media/PHAK%20-%20Chapter%2010.pdf
4. Ali J (2012) Wing Flaps for Lift Augmentation in Aircraft. Decoded Science.
5. http://en.wikipedia.org/wiki/Flap_%28aircraft%29
6. Schlüter JU (2009) Lift Enhancement at Low Reynolds Numbers using Pop-Up Feathers. 39th AIAA Fluid Dynamics Conference 22-25 June San Antonio, Texas, USA.
7. Ghoddoussi A (1998) A Conceptual Study of Airfoil Performance Enhancements Using CFD. Sojo University, Japan.
8. Ali J (2012) Slats, Slots and Spoilers—Lift Modifying Devices on Airplane Wings. Decoded Science.
9. Saha N (1999) Gap Size Effect on Low Reynolds Number Wind Tunnel Experiments. Blacksburg, Virginia USA.